PHYSICAL REVIEW A VOLUME 19, NUMBER 3 MARCH 1979

Theoretical and experimental study of the dynamic behavior of a nonlinear Fabry-Perot interferrometer

T. Bischofberger* and Y. R. Shen
Physics Department, University of California, Berkeley, California 94720
and Materials and Molecular Research Division, Lawrence Berkeley Laboratory, Berkeley, California 94720
(Received 28 September 1978)

We have studied theoretically and experimentally the dynamic behavior of a nonlinear Fabry-Perot interferrometer filled with a Kerr medium. The Fabry-Perot responses ranging from extremely transient to quasi-steady-state in various modes of operation are considered. The experimental results are in excellent agreement with theory. It is shown that the quasi-steady-state operation requires not only a medium response time much smaller than the cavity round-trip time, but also a characteristic time of the input intensity variation several hundred times larger than the cavity round-trip time. Even in the quasi-steady-state limit, optical switching is often featured by overshoot and ringing after switching. The switching speed is limited by the cavity buildup time.

I. INTRODUCTION

Recently, there has been growing interest in the physical understanding and possible applications of nonlinear Fabry-Perot (FP) interferrometry.[1] Seidel and Szoke *et al.* first proposed the use of a nonlinear absorbing FP interferrometer for optical limiting, discriminator, and bistable operations.[2] Later, McCall and coworkers successfully demonstrated such operations with sodium vapor or ruby as the nonlinear medium in the FP interferrometer cavity.[3] They pointed out, however, that their observations were actually dominated by the field-induced refractive index rather than the nonlinear absorption. Detailed theory of the steady-state operation of a nonlinear FP interferrometer filled with a purely refractive medium has already been worked out by Felber and Marburger.[4] More recently, various research groups have proposed and developed schemes that could lead to miniature nonlinear FP interferrometer for applications in integrated optical circuits.[5] Even mirrorless and integrated optical bistable devices have been demonstrated.[6] Theoretically, optical bistability has been discussed using analog to phase transition.[7] The quantum statistical properties and the spectrum of transmitted light of a bistable resonator have also been investigated.[8]

While the steady-state operation of a nonlinear FP interferrometer is now well understood, little attention, so far, has been paid to the dynamic behavior of a nonlinear FP interferrometer. In the practical design of a nonlinear FP interferrometer as an optical device, however, questions relating to the transient characteristics of the device, switching speed, etc., are clearly very important. We have recently reported the preliminary results of our theoretical and experimental study of the transient behavior of a nonlinear FP interferrometer filled with a Kerr liquid.[9] In this paper, we now give a complete theoretical analysis on how the nonlinear FP interferrometer behaves in its operation from the extremely transient case to the quasi-steady-state case as different characteristic parameters are varied.[10] We also show experimentally that our results obtained with an FP interferrometer filled with various Kerr media (liquid crystal, nitrobenzene, and CS_2) are in excellent agreement with the theoretical calculations.

We first review in Sec. II the theoretical formalism. We then describe, in Sec. III, the experimental arrangement and present, in Sec. IV, the experimental results in comparison with the theoretical calculations. In Sec. V, we extend the theoretical calculations of the bistable operation to the case with an ideal saw-tooth input pulse in order to discuss the transient operation characteristics of the nonlinear FP interferrometer more fully. We consider, in particular, the dependence of switching speed and ringing in the output on the various characteristic parameters. Finally, we discuss qualitatively the effect of transient response on the observed behavior of the nonlinear FP interferrometer reported by others.

II. THEORETICAL FORMALISM

We consider an FP interferrometer cavity filled with a Kerr medium. We assume that the field-induced refractive index Δn in the Kerr medium affects only the phase but not the amplitude of the field inside the cavity. Then, in the plane wave approximation with an input field $E_{in}(t) = \mathcal{E}_i(t) \exp(-i\omega t)$, the transmitted output field is

 ©1979 The American Physical Society

$$E_{\text{out}}(t)=Te^{-i\omega t}\sum_{m=0}^{\infty}\mathcal{E}_i\left[t-\left(m+\frac{1}{2}\right)t_R\right]\times R_\alpha^m e^{i\Phi[t,t-(m+1/2)t_R]} \quad (1)$$

$$=Te^{-i\omega t}\sum_{l=0}^{\infty}\sum_{m=0}^{l}\Delta\mathcal{E}_{il}R_\alpha^m e^{i\Phi[t,t-(m+1/2)t_R]},$$

where $\mathcal{E}_i[t-(m+\frac{1}{2})t_R]=\sum_{l=m}^{\infty}\Delta\mathcal{E}_{il}$ with $\Delta\mathcal{E}_{il}=\mathcal{E}_i[t-(l+\frac{1}{2})t_R]-\mathcal{E}_i[t-(l-\frac{1}{2})t_R]$, l and m are positive integers, t_R is the cavity round trip time, $R_\alpha=R\exp(-\alpha d)$, α is the attenuation coefficient in the cavity, d is the cavity length, R and T are the mirror reflection and transmission coefficients, respectively, and $\Phi[t,t-(m+\frac{1}{2})t_R]$ is the phase increment of the field entering the cavity at $t-(m+\frac{1}{2})t_R$ and leaving the cavity at t. If the variation of the field is small in t_R, then Eq. (1) can be approximated by

$$E_{\text{out}}(t)=Te^{-i\omega t}\int_{-\infty}^{t}\left(\frac{d}{dt'}\mathcal{E}_i(t')\right)\times\sum_{m=0}^{m_{\max}}R_\alpha^m e^{i\Phi[t,t-(m+1/2)t_R]}dt', \quad (2)$$

with $m_{\max}$ being an integer closest to but smaller than $(t-t')/t_R$.

The phase increment Φ is given by

$$\Phi\left[t,t-\left(m+\frac{1}{2}\right)t_R\right]=\sum_{l=0}^{m}\left(\frac{\omega}{c}\right)\left(\int_0^d\left\{n_0+\Delta n\left[t-\left(l+\frac{1}{2}\right)t_R+\left(\frac{c}{n_0}\right)z,z\right]\right\}dz+\sum_{l=1}^{m}\left(\frac{\omega}{c}\right)\int_d^0\left\{n_0+\Delta n\left[t-lt_R+\left(\frac{c}{n_0}\right)(d-z),z\right]\right\}dz\right). \quad (3)$$

Assuming the variation of Δn in a round trip time t_R is negligible, we can write

$$\Phi\left[t,t-\left(m+\frac{1}{2}\right)t_R\right]\cong\left(m+\frac{1}{2}\right)\phi_0+\frac{1}{2}\Delta\phi(t)+\sum_{l=1}^{m}\Delta\phi(t-lt_R), \quad (4)$$

where $\phi_0=(\omega/c)2n_0d$ and $\Delta\phi(t)=(\omega/c)\int\Delta n(t,z)dz$. The spatial variation of Δn arises from the interference of the forward and backward propagating waves in the cavity. It is sinusoidal and is therefore averaged out in the round-trip integral of $\Delta\phi$. For Kerr liquids, Δn and hence $\Delta\phi$ obey the Debye relaxation equation, namely,

$$\tau_D\frac{\partial\Delta\phi}{\partial t}+\Delta\phi=\frac{\omega d}{c}(\delta n_F+\delta n_B), \quad (5)$$

where τ_D is the Debye relaxation time, and δn_F and δn_B are the quasi-steady-state field-induced refractive indices seen by the forward and backward propagating waves E_F and E_B inside the cavity, respectively. Since the field-induced polarization in the medium is $P_{F,B}^{(3)}=(n_0/2\pi)n_2(|E_F|^2+|E_B|^2)E_{F,B}$, we have $\Delta n_{F,B}=(2\pi/n_0)\partial P_{F,B}^{(3)}/\partial E_{F,B}=2n_2|E_{F,B}|^2+n_2|E_{B,F}|^2$. Equation (5) then becomes

$$\tau_D\frac{\partial\Delta\phi}{\partial t}+\Delta\phi=\frac{3\omega dn_2}{c}(|E_F|^2+|E_B|^2). \quad (6)$$

The fields inside the cavity are related to E_{out} by $|E_{\text{out}}|^2=n_0T|E_F|^2=n_0T|E_B|^2/R$. Equation (6) can be written in the integral form as

$$\Delta\phi(t)=\frac{3\omega dn_2(1+R)}{n_0cT\tau_D}\int_{-\infty}^{t}|E_{\text{out}}(t')|^2e^{-(t-t')/\tau_D}dt'. \quad (7)$$

The coupled set of Eqs. (1), (4), and (7) now fully describe the dynamical property of the nonlinear FP interferrometer. They can be solved numerically on a computer using iterative self-consistent loops. A number of examples will be shown in Secs. IV and V. When the characteristic time T_c of the input intensity variation is much larger than τ_D and t_R, the operation of the FP interferrometer should become quasi-steady state. As expected, Eq. (1) then reduces to the well-known result

$$E_{\text{out}}=TE_{\text{in}}\exp[i(\phi_0+\Delta\phi)/2]/[1-R_\alpha\exp(i\phi_0+i\Delta\phi)] \quad (8)$$

and Eq. (7) becomes

$$\Delta\phi=[3\omega dn_2(1+R)/n_0cT]|E_{\text{out}}|^2. \quad (9)$$

In Secs. IV and V we shall discuss how large T_c should be relative to τ_D and t_R in order to assure the quasi-steady-state operation.

III. EXPERIMENTAL ARRANGEMENT

There are three important time constants in the problem: the characteristic time of input intensity variation T_c, the medium response time τ_D, and the cavity round-trip time t_R (or the cavity buildup time τ_c defined as $\tau_c = t_R/|1 - R_\alpha \exp(i\phi_0)|$). In our experiment, the input to the FP interferrometer was a laser pulse; so we can use the pulsewidth τ_p as the characteristic time T_c. With the Kerr medium in the FP interferrometer, τ_D is the Debye relaxation time. We wanted to consider in our experiment cases ranging from $\tau_D \gg \tau_p \gg t_R$ to $\tau_p > \tau_D > t_R$ to $\tau_p \gg t_R \gg \tau_D$, covering a wide range of the nonlinear FP interferrometer operation from the extremely transient to the quasi-steady state. In order to achieve this, we used three different Kerr media: a liquid crystalline material *n-p*-methoxybenzylidene-*p*-butylaniline (MBBA) in the isotropic phase, nitrobenzene, and CS_2. Because of its pretransitional behavior, MBBA has a relaxation time τ_D which can be easily varied by temperature.[11] Corresponding to a temperature variation from 65 °C to 45 °C, τ_D of MBBA varies from 15 to 174 nsec. Then, for nitrobenzene and CS_2, we have $\tau_D = 45$ and 2 psec at 20 °C, respectively. We also used two single-mode Q-switched ruby lasers with different pulsewidths $\tau_p = 14$ nsec and 62 nsec (full width at half-maximum), respectively. Both laser beams had a Gaussian beam profile with a radius of ~0.15 cm at the entrance of the FP interferrometer.

Our experimental setup is shown in Fig. 1. The FP interferrometer cavity was formed by two $\lambda/200$ plane mirrors with $R = 0.98$ separated by $d = 1$ cm. It was filled with one of the Kerr liquids and placed in a thermally controlled oven. The temperature of the FP interferrometer could be stabilized to within 10^{-3} °C. The linear round-trip phase shift ϕ_0 in the cavity was measured by an He-Ne laser beam and then modified to its value at the ruby laser frequency through calibration. For coarse adjustment of ϕ_0, the FP interferrometer was mechanically tuned, and for fine adjustment, thermally tuned. Because of the small attenuation loss due to scattering and absorption in the three Kerr liquids we used, the effective mirror reflectivity at the ruby laser frequency was $R_\alpha \simeq 0.78$. The experimentally determined finesse of the FP interferrometer was 13. Input and output laser pulses at the FP interferrometer were measured by fast photodiodes and displayed on two simultaneously triggered Tektronix 519 oscilloscopes. The input laser power was always kept well below the self-focusing threshold in the Kerr medium. Absolute laser intensities were obtained by measuring the laser power, the beam cross section, and the beam divergence at the entrance of the FP interferrometer. The measured peak laser intensities were accurate to within 15%.

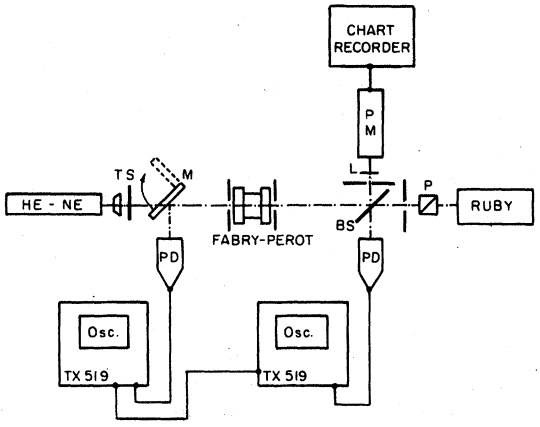

FIG. 1. Schematic diagram of the experimental setup. P: polarizer; BS: beamsplitters; L: lense; M: movable mirror; TS: telescope; PD: photodiode; PM: photomultiplier.

IV. EXPERIMENTAL RESULTS AND COMPARISON TO THEORY

Our measurements with different pulse intensities were made at FP interferrometer phase detunings $\Delta\phi_0 = 0$, -0.1π, and -0.2π rad ($\phi_0 = \Delta\phi_0$ + multiple of 2π). These values of $\Delta\phi_0$ were chosen such that the steady-state operation of the nonlinear FP interferrometer are in three different distinct modes, e.g., the power limiter, the differential gain, and the bistable mode respectively. Figure 2 shows three typical examples for each value of $\Delta\phi_0$. The dots are obtained from the measured oscilloscope traces. The plots on the right-hand side of Fig. 2 give I_{out} vs I_{in} with time t as the varying parameter. The solid curves are the theoretical curves. We first fit the measured $I_{in}(t)$ by a Gaussian pulse. Then, using Eqs. (1), (3), and (7), we calculated $I_{out}(t)$ and $\Delta\phi(t)$. The self-consistent calculation was carried out with the difference of $\Delta\phi$ between two final successive iteration steps less than 1 mrad. One normalization constant was used to fit the peak of $I_{out}(t)$ in Fig. 2(a), and then, the same normalization constant was used for calculating $I_{out}(t)$ and $\Delta\phi(t)$ in Figs. 2(b) and 2(c). Furthermore, the calculated $I_{out}(t)$ also took into account the response time of the detector system through convolution with the detector response function. The same procedure was taken in calculating the curves in Figs. 3–8. In all cases, we find excellent agreement between theory and experiment.

Figures 2–8 show progressively how $I_{out}(t)$,

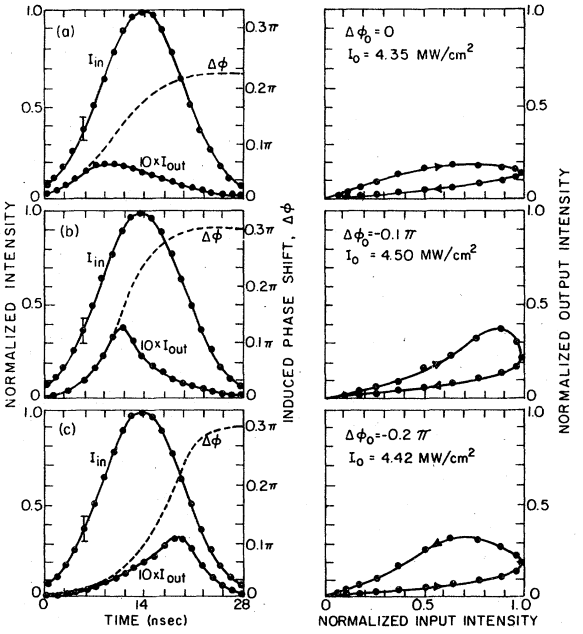

FIG. 2. $I_{in}(t)$, $I_{out}(t)$, $\Delta\phi(t)$, and I_{out} vs I_{in} for $t_R < \tau_p \ll \tau_D$ with $t_R = 0.11$ nsec, $\tau_p = 14$ nsec, and $\tau_D = 145$ nsec. The FP interferrometer cavity is filled with MBBA. The curves are calculated from Eqs. (1), (4), and (7), while the dots are obtained from measurements. Three modes of operation are presented here, (a) power limiter, (b) differential gain, and (c) bistability.

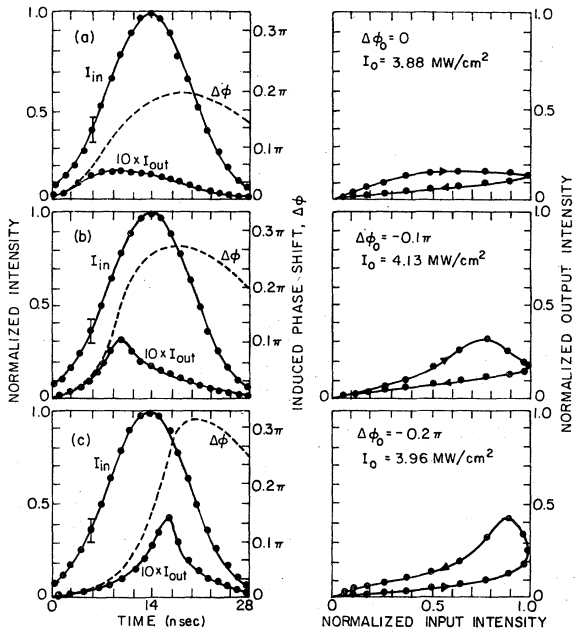

FIG. 4. $t_R < \tau_p \approx \tau_D$ with $t_R = 0.11$ nsec, $\tau_p = 14$ nsec, and $\tau_D = 15$ nsec. Others are the same as in Fig. 2.

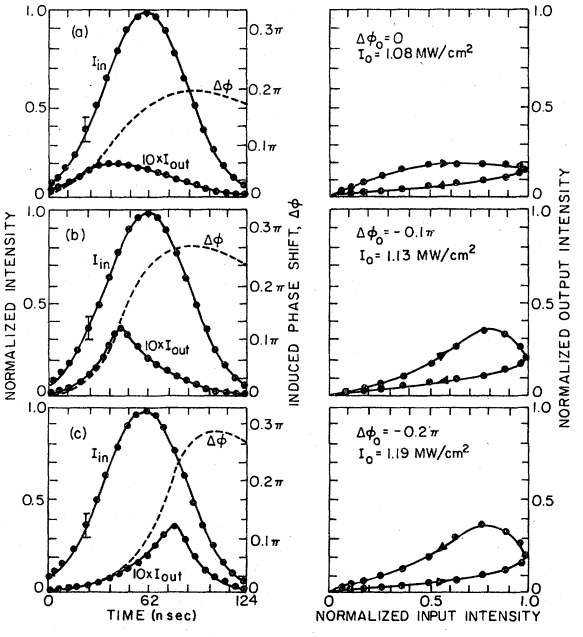

FIG. 3. $t_R < \tau_p < \tau_D$ with $t_R = 0.11$ nsec, $\tau_p = 62$ nsec, and $\tau_D = 145$ nsec. Others are the same as Fig. 2.

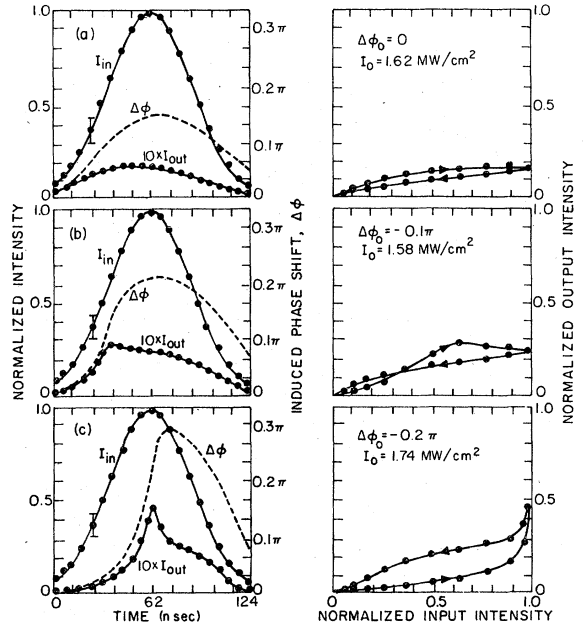

FIG. 5. $t_R < \tau_D < \tau_p$ with $t_R = 0.11$ nsec, $\tau_p = 62$ nsec, and $\tau_D = 15$ nsec. Others are the same as Fig. 2.

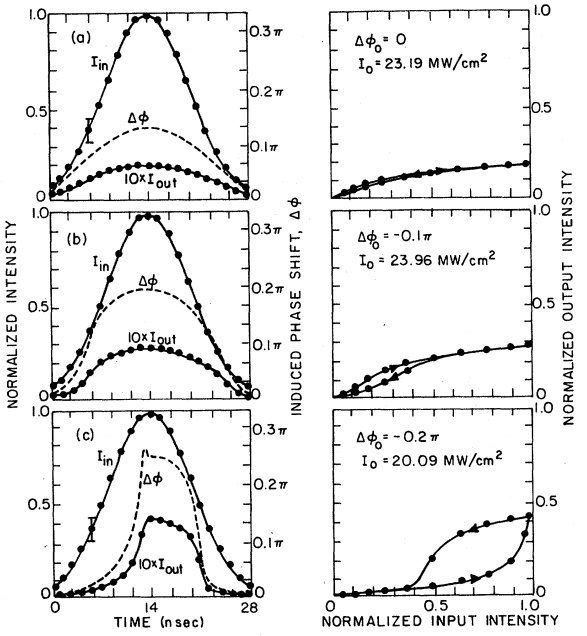

FIG. 6. $\tau_D < t_R < \tau_p$ with $t_R = 0.10$ nsec, $\tau_p = 14$ nsec, and $\tau_D = 45$ psec. The FP interferrometer cavity is filled with nitrobenzene. Others are the same as in Fig. 2.

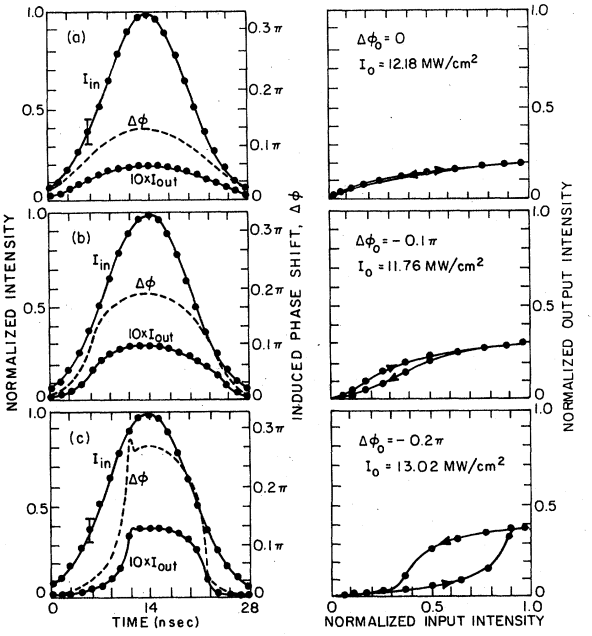

FIG. 7. $\tau_D \ll t_R < \tau_p$ with $t_R = 0.11$ nsec, $\tau_p = 14$ nsec, and $\tau_D = 2$ psec. The FP interferrometer cavity is filled with CS_2. Others are the same as in Fig. 2.

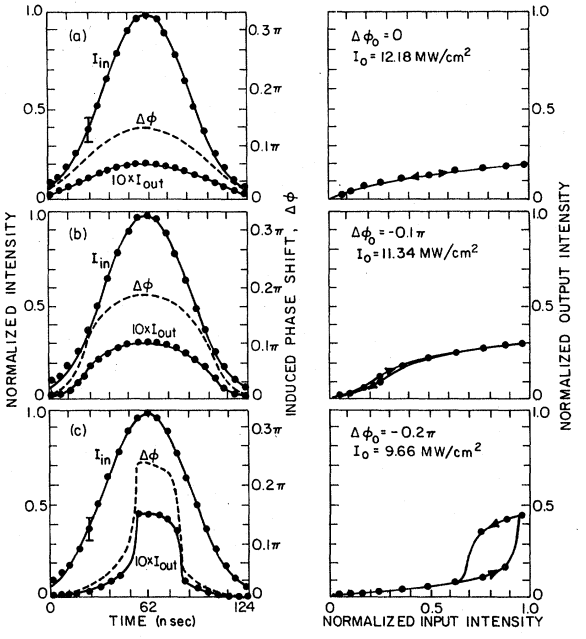

FIG. 8. $\tau_D \ll t_R < \tau_p$ with $t_R = 0.11$ nsec, $\tau_p = 62$ nsec, and $\tau_D = 2$ psec. The FP interferrometer cavity is filled with CS_2. Others are the same as in Fig. 2.

$\Delta\phi(t)$, and $I_{out}(t)$ vs $I_{in}(t)$ vary when the molecular relaxation time τ_D decreases from $\tau_D \gg \tau_p \gg t_R$ to $\tau_D \ll t_R \ll \tau_p$. When $\tau_D \geq t_p$ (Figs. 2–5), the curves of $\Delta\phi(t)$ show clearly the transient response of the medium to the cavity field, but when $\tau_D \ll t_p$ (Figs. 6–8), the medium responds to the field almost instantaneously, and $\Delta\phi(t)$ becomes essentially proportional to $I_{out}(t)$. The variation from the transient to the quasi-steady-state operation of the FP interferrometer can also be easily seen in Figs. 2–8. In the power-limiter mode ($\Delta\phi_0 = 0$), I_{out} vs I_{in} first appears as a loop in the transient case, and gradually shrinks to a line as the operation becomes less and less transient. In the differential gain mode ($\Delta\phi_0 = -0.1\pi$rad), a similar but more easily visualized transformation takes place with I_{out} vs I_{in} eventually showing the S-type characteristic curve in the quasi-steady-state limit. The bistable mode of operation ($\Delta\phi_0 = -0.2\pi$ rad) displays the transition from transient to quasi-steady state most dramatically. In the transient limit [Figs. 2(c) and 3(c)], I_{out} vs I_{in} is also in the form of a loop, even though the circulation around the loop is counterclockwise, opposite to that appearing in the power limiter and differential gain cases. Then, it begins to appear like a hysteresis loop in Figs. 4(c) and 5(c), and finally transforms into such a loop towards the quasi-steady-state limit in Figs. 6(c)–8(c).

We note that even in Figs. 6 and 7, with $\tau_p/\tau_D = 310$ and 7000, respectively, the curves exhibit some transient characteristics. This is because in these two cases even though the material response can be considered as instantaneous, $\tau_p/t_R = 140$ is not large enough so that the cavity field buildup is still somewhat transient. With a longer input laser pulse in Fig. 8 corresponding to $\tau_p/t_R = 620$, the transient effect is clearly reduced. Even in the quasi-steady state, the optical switching of the bistable operation mode occuring in a time comparable to t_R would show some transient phenomenon in the form of overshoot and ringing.[9] In our experimental observation, however, they are partially masked by the slow response of our detection system. The overshoot and ringing effects could be important in the applications of fast optical switching. We shall therefore discuss theoretically these effects as well as the switching speed in Sec. V.

V. DYNAMIC BEHAVIOR OF OPTICAL BISTABILITY

In order to exhibit more clearly the transient characteristics of the bistable operation, we also performed theoretical calculations using a triangular input pulse. The results are shown in Figs. 9–11 with the detuning of the FP interferrometer set at $\Delta\phi_0 = -0.4\pi$. In Fig. 9, three different values of τ_p ($250t_R$, $100t_R$, and $50t_R$) are used while the other parameters such as the Debye relaxation time τ_D ($=0.01t_R$), the mirror reflectivity R ($=70\%$), and the input peak intensity I_{in} (normalized to 1) are kept constant. Since we have $\tau_p > t_R \gg \tau_D$, the medium response in this case is essentially instantaneous. The transient effect therefore arises from the finite time required for the cavity field buildup. As shown in Fig. 9, the transient effect in the sense of slowing down of the switching speed is quite obvious even at $\tau_p/t_R = 100$ and only becomes negligible when $\tau_p/t_R \geq 250$. Then, the overshoot and ringing after switching are also more clearly displayed with longer ringing periods in the more transient cases. Physically, overshoot and ringing after switching can be easily understood. As is well known, field in a resonant cavity cannot make sudden finite changes. It has to approach the final value through interference of multiple reflections. When the finesse (or the Q factor) of the cavity is sufficiently large, we have then the underdamped and ringing situation. We also expect to have more ringing in a cavity with a larger finesse. In the quasi-steady state with $\tau_p \gg t_R \gg \tau_D$, the ringing should be over in roughly two cavity buildup times (τ_c). If we consider optical switching as completed when the ringing is over, then the switching time is limited by a few τ_c even in the quasi-steady-state operation.

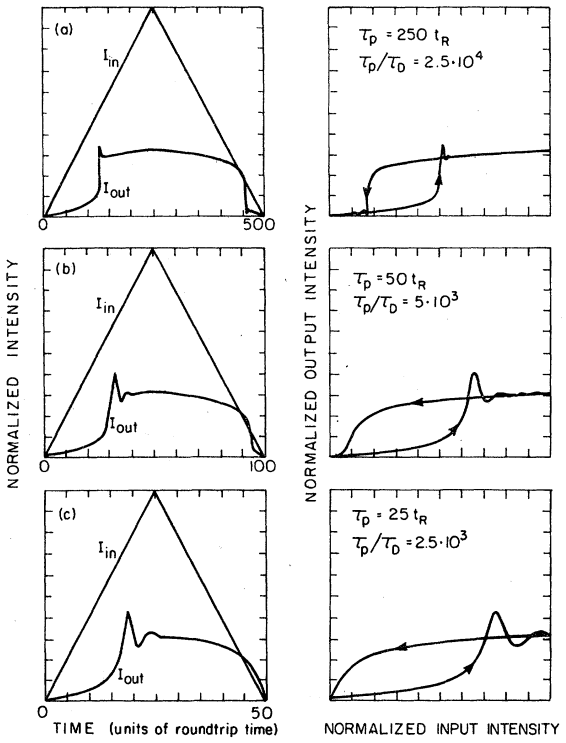

FIG. 9. $I_{in}(t)$, $I_{out}(t)$, and I_{out} vs I_{in} of the bistable model of operation calculated for three different pulse durations τ_p with $\Delta\phi_0 = -0.4\pi$, $\tau_D = 0.01t_R$, $R_\alpha = 70\%$, and the normalized input peak intensity kept constant. Note the different time scales in the figures on the left.

In Fig. 10, we show the effect of the finite medium response time on the switching behavior. Three examples are given with $\tau_D = 0.01t_R$, $2.5t_R$, and $25t_R$ and the other parameters kept constant. Clearly, even when $\tau_p/\tau_D = 100$, the transient switching characteristic in the form of slow switching and ringing is still obvious. This is mainly because $\tau_D \geq t_R$ so that the material response slows down the cavity field buildup. Therefore, the quasi-steady-state case is expected to set in only when $\tau_D < t_R$ and $\tau_p/t_R \geq 250$.

In the quasi-steady-state limit where $\tau_p \gg t_R \gg \tau_D$, the reflectivity of the FP interferrometer mirrors will finally set the switching speed and affect overshoot and ringing. We show the effect of mirror reflectivity in Fig. 11. As seen in Fig. 11, lower mirror reflectivity slows down in switching speed and damps out the overshoot and ringing. The apparently slower switching is due to the smoother and broader FP interferrometer transmission curve at lower R, while the stronger damping on the ringing arises from the lower finesse

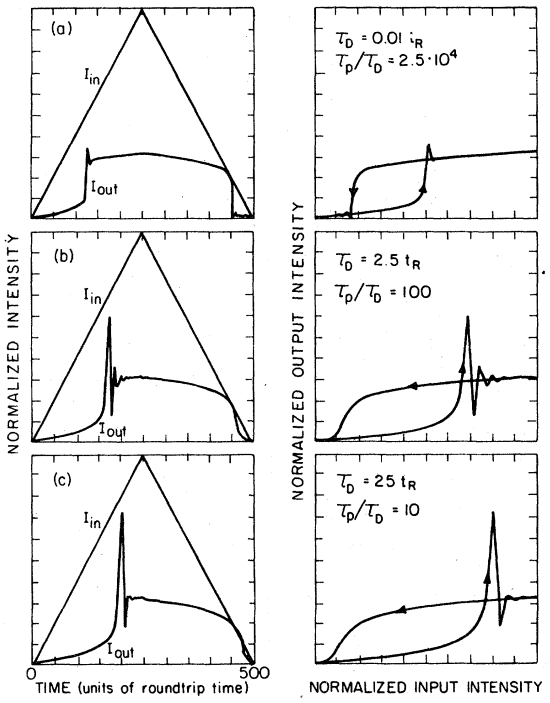

FIG. 10. $I_{in}(t)$, $I_{out}(t)$, and I_{out} vs I_{in} of the bistable mode of operation for three different molecular relaxation times τ_D with $\Delta\phi_0 = -0.4\pi$, $\tau_p = 250 t_R$, $R_\alpha = 70\%$ and the input peak intensity kept constant.

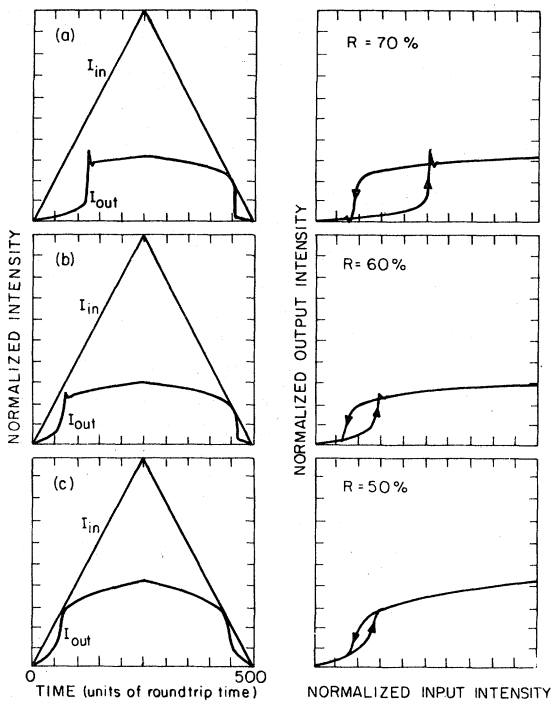

FIG. 11. $I_{in}(t)$, $I_{out}(t)$, and I_{out} vs I_{in} of the bistable model of operation for three different effective mirror reflectivities R_α with $\Delta\phi_0 = -0.4\pi$, $\tau_D = 0.01 t_R$, $\tau_p = 250 t_R$, and the input peak intensity kept constant.

of the cavity.

From the above results, we can therefore conclude that in order to have a sharp optical switching, we need a cavity with a higher finesse, but then overshoot and ringing after switching will be more obvious. The switching speed is fastest in the quasi-steady-state limit ($\tau_p \gg t_R \gg \tau_D$) and is limited by the cavity buildup time.

The theoretical discussion here can be qualitatively extended to the experimental observations reported by others, although the equation governing the material response may be different in different cases. For example, Smith *et al.*[5] used a nonlinear FP interferrometer in which the nonlinear phase shift was provided by an electro-optical crystal driven by the transmitted or reflected light. In that case, the material response was dominated by the response time $\tau_F \simeq 1$ nsec of the electronic feedback system, i.e., τ_F plays the role of τ_D. Using $\tau_D \equiv \tau_F = 1$ nsec, $t_R \simeq 1$ nsec, $R_\alpha \simeq 63\%$, and $\tau_p \gg t_R \sim \tau_D$ in our calculation, we can actually obtain a set of I_{out} vs I_{in} curves for the various modes of operation (corresponding to different $\Delta\phi_0$) very similar to what Smith *et al.* have observed.

Grischkowsky[12] has studied the bistable mode of operation of a nonlinear FP interferrometer filled with Rb vapor. The characteristic parameters in his case are $t_R = 30$ psec, $\tau_D = 200$ psec, $\tau_p = 7$ nsec, $R_A = 0.73$, and $\Delta\phi_0 = -0.24$ rad. Since $\tau_D > t_R$ even though $\tau_p/t_R = 230 \gg 1$, the transient response of the FP interferrometer should be quite obvious. The output should resemble the I_{out} curve in Fig. 10(c). An actual calculation taking into account the finite response time (~1 nsec) of the detection system and the true input pulseshape can in fact reproduce the observed $I_{out}(t)$ quite well.

Overshoot and ringing in optical switching of a FP interferrometer has been mentioned by Smith. They can, in fact, also be seen in the bistable operation of the mirrorless feedback scheme as reported by Feldman.[6]

VI. CONCLUSION

We have presented here the results of a detailed theoretical and experimental study of the dynamic behavior of a nonlinear FP interferrometer filled with a Kerr medium. The three modes of operation, namely, power limiter, differential gain, and optical bistability, are considered. The ex-

perimental results covering a wide range from the extremely transient to the quasi-steady-state case are all in excellent agreement with theory. We show that in order to have quasi-steady-state operation, the characteristic time of the input intensity variation must be several hundred times the cavity round-trip time which should in turn be larger than the material response time. Even in the quasi-steady-state limit, optical switching in the bistable mode of operation is still often characterized by overshoot and ringing as the cavity field makes underdamped adjustment from its initial value to the final value. The optical switching speed is then limited by the cavity buildup time. Switching is less sharp and ringing is more highly damped if the FP interferrometer cavity has a lower finesse. Although our theoretical calculation is restricted to FP interferrometry with a Kerr medium, the results are still valid in a qualitative sense for the other types of nonlinear FP interferrometer.

ACKNOWLEDGMENTS

One of the authors (T. B.) was supported by the Division of Materials Sciences, Office of Basic Energy Sciences, U. S. Department of Energy and the other (Y. R. S.) was supported by the NSF under Grant No. 76-19843.

---

*Present address: Solid State Physics Laboratory, Swiss Federal Institute of Technology (ETH), CH-8093, Zurich, Switzerland.

[1]See, for example, papers presented in the Tenth International Quantum Electronics Conference, Atlanta, Georgia, June 1978 (unpublished).

[2]H. Seidel, U. S. Patent No. 3 610 731; A. Szöke, V. Danean, J. Goldhar, and N. A. Kurnit, Appl. Phys. Lett. 15, 376 (1969); A. Szöke, U. S. Patent No. 3 813 605; E. Spiller, J. Appl. Phys. 43, 1673 (1972); J. W. Austin and L. G. DeShazer, J. Opt. Soc. Am. 61, 650 (1971).

[3]S. L. McCall, Phys. Rev. A 9, 1515 (1974); S. L. McCall, H. M. Gibbs, and T. N. C. Venkatesan, J. Opt. Soc. Am. 65, 1184 (1975); H. M. Gibbs, S. L. McCall, and T. N. C. Venkatesan, Phys. Rev. Lett. 36, 1135 (1976); T. N. C. Venkatesan and S. L. McCall, Appl. Phys. Lett. 30, 282 (1977); H. M. Gibbs, S. L. McCall, and T. N. C. Venkatesan, U. S. Patent No. 4 012 699.

[4]F. S. Felber and J. H. Marburger, Appl. Phys. Lett. 28, 731 (1976); J. H. Marburger and F. S. Felber, Phys. Rev. A 17, 335 (1978).

[5]M. Okuda, M. Togota, and K. Ouaka, Opt. Commun. 19, 138 (1976); M. Okuda and K. Ouaka, Jap. J. Appl. Phys. 16, 769 (1977); P. W. Smith and E. H. Turner, Appl. Phys. Lett. 30, 280 (1977); P. W. Smith, E. H. Turner, and P. J. Maloney, IEEE J. Quant. Elec. QE-14, 207 (1978); P. W. Smith, E. H. Turner, and B. B. Mumford, Optics Lett. 2, 55 (1978).

[6]E. Garmire, J. H. Marburger, and S. D. Allen, Appl. Phys. Lett. 32, 320 (1978); A. Feldman, Appl. Phys. Lett. 33, 243 (1978); P. W. Smith, I. P. Kaminow, P. J. Maloney, and L. W. Stulz, Appl. Phys. Lett. 33, 24 (1978).

[7]R. Bonafacio and L. A. Lugiato, Opt. Commun. 19, 172 (1976); L. M. Narducci and R. Gilmore, in Proceedings of the Fourth Rochester Conference on Coherence and Quantum Optics, June 1977, edited by L. Mandel and E. Wolf (unpublished); L. A. Lugiato, P. Mandel, S. T. Dembinski, and A. Kossakowski, Phys. Rev. 18, 238 (1978).

[8]R. Bonifacio and L. A. Lagiato, Phys. Rev. Lett. 40, 1023 (1978); G. S. Agarwal, L. M. Narducci, D. H. Feng, and R. Gilmore (unpublished).

[9]T. Bischofberger and Y. R. Shen, Appl. Phys. Lett. 32, 156 (1978).

[10]Preliminary results were presented in the Ref. 1.

[11]G. K. L. Wong and Y. R. Shen, Phys. Rev. A 10, 1277 (1974).

[12]D. Grischkowski, in Ref. 1, Paper F.3.